DALTON
FULL PAPER

Mono- and di-nuclear complexes of the ligands 3,4-di(2-pyridyl)-1,2,5-oxadiazole and 3,4-di(2-pyridyl)-1,2,5-thiadiazole; new bridges allowing unusually strong metal–metal interactions

Chris Richardson,[a] Peter J. Steel,*[a] Deanna M. D'Alessandro,[b] Peter C. Junk[b] and F. Richard Keene*[b]

[a] *Department of Chemistry, University of Canterbury, Christchurch, New Zealand*
[b] *School of Pharmacy & Molecular Sciences, James Cook University, Townsville, Queensland 4811, Australia. E-mail: Richard.Keene@jcu.edu.au*

Received 23rd March 2002, Accepted 1st May 2002
First published as an Advance Article on the web 29th May 2002

The syntheses of two new ligands, 3,4-di(2-pyridyl)-1,2,5-oxadiazole (dpo) and 3,4-di(2-pyridyl)-1,2,5-thiadiazole (dpt), are described. Complexes with palladium and copper have seven-membered chelate rings with coordination through the two pyridine nitrogens, whereas in the silver nitrate complex of dpt the ligand acts as a bridge between metal centres. Studies of the mononuclear ruthenium complexes indicate five-membered chelate rings (involving donor nitrogen atoms from each of a pyridine ring and the oxadiazole or thiadiazole ring) and reveal that these ligands are very electron deficient and possess very low energy π* orbitals. Dinuclear ruthenium complexes have been prepared and the diastereoisomers separated and crystallographically characterised. Electrochemical studies of these complexes reveal remarkably strong metal–metal interactions, which also depend on the stereoisomeric form. Some heterodinuclear complexes have also been prepared.

Introduction

Ruthenium(II) complexes involving polypyridyl ligands have attracted significant recent interest, motivated largely by their potential as the basis of novel functional materials.[1,2] In particular, polymetallic assemblies based on such centres have elicited attention because of their multicomponent nature, and the electrochemical, photochemical and photophysical properties of such species have been widely investigated.[3] For a majority of the complexes studied, the metal centres are linked by a ligand bridge, and the nature of the bridge has a fundamental influence on the electronic interaction between the metals and therefore on the characteristics of the material.

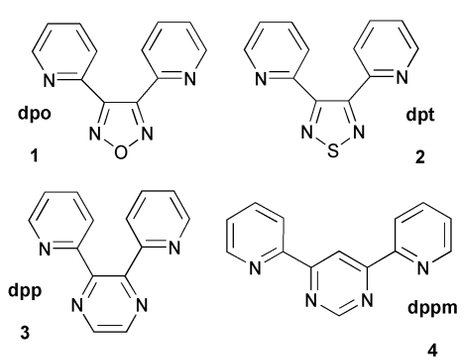

The ligands 3,4-di(2-pyridyl)-1,2,5-oxadiazole (dpo; **1**) and 3,4-di(2-pyridyl)-1,2,5-thiadiazole (dpt; **2**) are the subject of the present investigation. They have a structural similarity to 2,3-di(2-pyridyl)pyrazine (dpp; **3**), and 4,6-di(2-pyridyl)pyrimidine (dppm; **4**), both of which have been widely studied.[3–5] In dinuclear complexes involving ligand **3**, the pyridine rings of the ligand are tilted with respect to the central pyrazine ring because of the steric clash between the H3 protons of the pyridyl rings. This leads to disruption of overlap of the π-systems within the ligand. Even so, dinuclear ruthenium complexes of **3** exhibit metal–metal interactions, exemplified by the difference in the redox couples of the two Ru(II)/Ru(III) oxidation processes (ΔE = 170 mV).[6] Ligand **4** is a sterically less demanding ligand than **3**: the pyridyl rings of the ligand are further separated, leading to reduced steric interaction, which enhances the stability of dinuclear complexes. Ligand **4** also leads to a shorter metal–metal distance than **3** but, despite these favourable features, the metal–metal interaction in dinuclear ruthenium complexes of **4** is slightly less (ΔE = 160 mV).[5]

Replacing the central six-membered diazine rings with a five-membered heterodiazole has some important consequences geometrically and electronically. Firstly, the internal angle within a five-membered ring is greater than that in a six-membered ring (72° *vs.* 60°), which should reduce the steric interaction between pyridine rings for the dinuclear complexes of **1** and **2** relative to those encountered in the dinuclear complexes with ligand **3**. Another favourable outcome of replacing the central six-membered ring with a five-membered ring is that the distance across the five-membered ring is less. This will result in the metal–metal distance being decreased relative to dinuclear complexes containing **3** and comparable to those containing **4**. These differences may impose significantly different properties to the dinuclear complexes of **1** and **2** relative to those of **3** and **4**.

Previous studies of the coordination chemistry of 1,2,5-heterodiazoles have been mainly restricted to 2,1,3-benzothiadiazoles[7–9] and their simple derivatives.[10,11] In particular, various groups[8,12] have investigated metallopolymeric networks derived from simple 2,1,3-benzothiadiazoles and Cu(II) salts. A study by Kaim *et al.*[13] examined the properties of dinuclear molybdenum pentacarbonyl complexes bridged by 2,1,3-benzothiadiazole and 2,1,3-benzoselenadiazole rings. The coordination chemistry of 1,2,5-oxadiazoles has been even less well investigated with only one report in the literature.[14] Accordingly, all of the reported studies on the 1,2,5-heterodiazole systems have been of simple monocyclic ligands and not those capable of a chelating coordination mode. The present study is

DOI: 10.1039/b202954e

directed to these heterocycles incorporated into new chelating heterocyclic ligands. We describe the synthesis and characterisation of the ligands **1** and **2**, together with their mononuclear ruthenium, palladium, copper and silver complexes, homodinuclear ruthenium complexes, and heterodinuclear ruthenium–palladium and ruthenium–platinum complexes.

Results and discussion

Ligand syntheses

Two well-established procedures exist for the synthesis of 1,2,5-oxadiazoles — the cyclodehydration of α-dioximes and the deoxygenation of 1,2,5-oxadiazole-2-oxides.[15] Using the former procedure, ligand **1** was produced in two steps starting from commercially available 2,2′-pyridil, as shown in Scheme 1. An

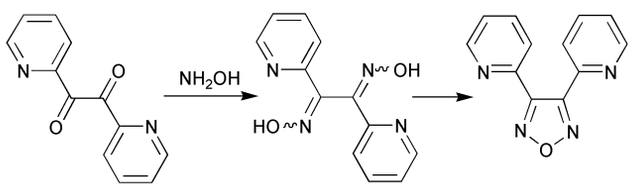

Scheme 1

α-dioxime was prepared, in 52% yield, by reacting the diketone with an excess of aqueous hydroxylamine, and subsequent heating of the dioxime at 185 °C for 18 hours in a sealed tube effected cyclization, in 44% yield, to give the new ligand **1**, which was characterised by melting point, ^{1}H and ^{13}C NMR spectroscopy, EI mass spectrometry and elemental analysis.

Several synthetic methodologies are available for 1,2,5-thiadiazoles,[16] the most general of which has been the action of disulfur dichloride (S_2Cl_2) on α-diamines or dioximes.[17] Rees *et al.*[18] have recently described a new method for the synthesis of 1,2,5-thiadiazoles based on reactions of the inorganic heterocycle trithiazyl trichloride ($S_3N_3Cl_3$) with alkenes and alkynes. This reaction is applicable to a wide range of substrates,[19–24] and, by retrosynthetic analogy, reaction of 1,2-di(2-pyridyl)-ethene should lead to the desired thiadiazole-containing dpt (**2**).

1,2-Di(2-pyridyl)ethene was prepared by refluxing 2-methylpyridine with pyridine-2-carboxaldehyde in the presence of acetic anhydride, as described by Newkome *et al.*[25] In the ligand synthesis (Scheme 2), a suspension of $S_3N_3Cl_3$ in dry toluene

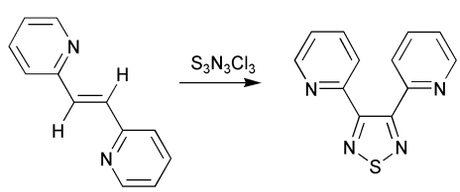

Scheme 2

was added dropwise with stirring to 1,2-di(2-pyridyl)ethene dissolved in a mixture of dry pyridine and dry toluene. The solution turned green and a precipitate formed; the mixture was refluxed for 18 hours before the reaction was stopped and the product isolated in 49% yield. The new 1,2,5-thiadiazole-containing ligand was characterised by melting point, ^{1}H and ^{13}C NMR spectroscopy, EI mass spectrometry and elemental analysis.

Mononuclear complexes

Ruthenium species. The bis(heteroleptic) species $[Ru(bpy)_2(dpo)]^{2+}$, $[Ru(Me_2bpy)_2(dpo)]^{2+}$ and $[Ru(bpy)_2(dpt)]^{2+}$ were straightforward in terms of their syntheses and characteristics. They were obtained as the hexafluorophosphate salts in high yield (*ca.* 90%) by reaction of the ligands **1** and **2** with one equivalent of $[Ru(bpy)_2Cl_2]$ {or $[Ru(Me_2bpy)_2Cl_2]$} in 3 : 1 ethanol–water. NMR studies of $[Ru(bpy)_2(dpo)]^{2+}$ using the 1-D TOCSY (Total Correlation Spectroscopy) technique identified six different rings in the complex, consistent with the attachment of the nitrogen of a pyridine ring and N2 of the oxadiazole, with the ligand having an uncoordinated pyridine ring (Fig. 1). Unlike the other H6 protons, the H6 of the

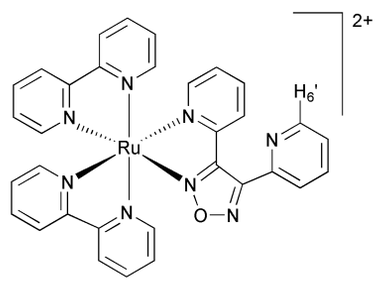

Fig. 1 Structure and proposed conformation of $[Ru(bpy)_2(dpo)]^{2+}$.

uncoordinated ring (H6′) experiences no ring-current anisotropy effects and is very much downfield of the others at the chemical shift of 9.03 ppm. The other distinctive proton in the spectrum is at 9.86 ppm and is assigned as H3 of the coordinated pyridine ring of the oxadiazole-containing ligand. This assignment was based upon the assumption that the pyridine nitrogen of the uncoordinated ring deshields this proton. Therefore, the conformation in solution is one where the uncoordinated ring lies in the same plane as the chelate ring with the nitrogen atom pointing towards H3 of the coordinated ring (Fig. 1). Confirmation that these were indeed the rings of the oxadiazole-containing ligand was obtained by the preparation of the analogous $[Ru(Me_2bpy)_2(dpo)](PF_6)_2$ complex. The NMR characteristics of $[Ru(bpy)_2(dpt)]^{2+}$ were consistent with those of the dpo analogue (see Experimental section).

The electrochemistry of the complexes reveal that the redox potentials associated with the Ru(III)/Ru(II) oxidation are more anodic than observed for $[Ru(bpy)_3]^{n+}$ (1.29 V *vs.* SCE),[26] indicating that the dpo and dpt ligands are electron-deficient and are involved in π-backbonding with the metal centre — to a lesser extent with dpt than dpo. The electronegative oxygen atom in complexes $[Ru(bpy)_2(dpo)]^{2+}$ and $[Ru(Me_2bpy)_2(dpo)]^{2+}$ acts to reduce the electron density of the ruthenium atom, raising the potential for oxidation of the complex to 1.51 and 1.40 V, respectively. The explanation for the redox potential (+1.37 V) associated with oxidation of $[Ru(bpy)_2(dpt)]^{2+}$ is that the sulfur is less electronegative than oxygen, and does not reduce the electron density of the metal to the same extent. A recent study[27] determined that the 1,2,5-oxadiazole system was the least delocalised of the isomeric oxadiazoles, and postulated that the electronegative oxygen atom prevents the electrons in its p_Z orbital from interacting effectively with the rest of the π-electron system of the ring. Consequently, the 1,2,5-oxadiazole system appears to have a high diene character. Perhaps it can be expected that the thiadiazoles are more 'aromatic' than oxadiazoles, in the same way that thiophene is more aromatic than furan.

Both $[Ru(bpy)_2(dpo)]^{2+}$ and $[Ru(Me_2bpy)_2(dpo)]^{2+}$ had an irreversible first reduction which, based upon the potential, is assigned to the dpo ligand. In contrast, the dpt complex underwent a reversible first reduction process.

The homoleptic ruthenium complexes $[Ru(dpo)_3]^{2+}$ and $[Ru(dpt)_3]^{2+}$ were also synthesised. For such tris(bidentate) species in which the ligands are unsymmetrical, meridional (*mer*) and facial (*fac*) geometric isomers are possible in addition to chiral (Λ and Δ) forms. Typically, when there are no significant differences in steric interactions between the *mer*- and *fac*- isomers, they would be expected to form in a statistical ratio of 3 : 1.

The ligands dpo and dpt were reacted with $[Ru(DMSO)_4Cl_2]$ in 3 : 1 ethanol–water. The desired homoleptic complexes, $[Ru(dpo)_3](PF_6)_2$ and $[Ru(dpt)_3](PF_6)_2$, were isolated and purified *via* the usual procedures: $[Ru(dpt)_3](PF_6)_2$ was characterised by FAB-MS and elemental analysis and $[Ru(dpo)_3](PF_6)_2$ by FAB-MS. The ^{1}H NMR spectrum of $[Ru(dpt)_3](PF_6)_2$ revealed the geometric isomers were not formed in the 3 : 1 ratio. The spectrum of the isomeric mixture was not assigned in detail; however, the H3 protons of the coordinated pyridine rings were downfield (*ca.* 8.9 ppm), so that it seems the same phenomenon of deshielding observed in the ^{1}H NMR identification of $[Ru(bpy)_2(dpt)](PF_6)_2$ is also present for each of the ligands in the complex $[Ru(dpt)_3](PF_6)_2$. Attempts were made to separate the geometric isomers of $[Ru(dpo)_3]^{2+}$ using the cation-exchange techniques established in our laboratories,[28] but they were not successful and were not pursued as the issue was not central to the thrust of the work.

Electrochemical measurements were made on these homoleptic complexes: no oxidation process of the ruthenium was observed for either $[Ru(dpt)_3](PF_6)_2$ or $[Ru(dpo)_3](PF_6)_2$ within the anodic limit of the experiment (+2.0 V), highlighting the electron-deficient nature of the ruthenium atom in these complexes as a consequence of the low π* level of the ligands. The redox potentials for the Ru(II)/Ru(III) oxidation of the complexes $[Ru(dpp)_3]^{2+}$ and $[Ru(dppm)_3]^{2+}$ occur at +1.68 and +1.39 V, respectively under the same conditions,[5,26] emphasising the electron deficiency of dpo and dpt relative to dpp and dppm. Upon scanning to cathodic potentials, the complexes each underwent one irreversible redox process: for $[Ru(dpt)_3](PF_6)_2$ at −0.73 V, and for $[Ru(dpo)_3](PF_6)_2$ at −0.41 V. These are compared with analogous (reversible) ligand-based reductions for $[Ru(dpp)_3]^{2+}$ (−0.95 V) and $[Ru(dppm)_3]^{2+}$ (−0.99 V),[5,26] which also attest to the low π* energy values of dpt and, in particular, dpo.

Palladium, copper and silver species. Palladium(II) complexes of dpo and dpt were prepared by reacting the ligand with $Li_2[PdCl_4]$ in methanol; yellow complexes were obtained in high yields (95 and 90%, respectively). These each analysed with 1 : 1 stoichiometry: $[Pd(L)Cl_2]$. The ^{1}H NMR spectra (recorded in d_6-DMSO) showed the presence of both coordinated and free ligand, indicating partial dissociation of the complexes. However, the spectra of the complexes showed signals for just one pyridine ring, indicating symmetrical coordination of the ligand. Furthermore, comparison of the chemical shifts of the free and complexed ligands revealed coordination-induced downfield shifts that were very similar to those observed in the previously characterised palladium(II) complex of the *N*-oxide of dpo.[29] From these facts we conclude that the ligands coordinate to the palladium through the two pyridine nitrogen atoms, with the formation of a seven-membered chelate ring, as shown in Fig. 2 for $[Pd(dpo)Cl_2]$. A similar dichloroplatinum

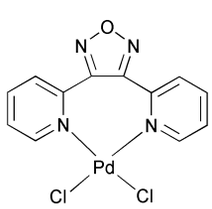

Fig. 2 Proposed structure of $[Pd(dpo)Cl_2]$.

complex of dpt was also prepared in 91% yield, but this proved to be insoluble in all common solvents.

The ligand dpt was then reacted with two equivalents of copper(II) nitrate in methanol — initially with the aim of synthesising a dinuclear species. However, the product was mononuclear, and sky-blue crystals suitable for crystallography were afforded directly from the reaction mixture. The structure is shown in Fig. 3.

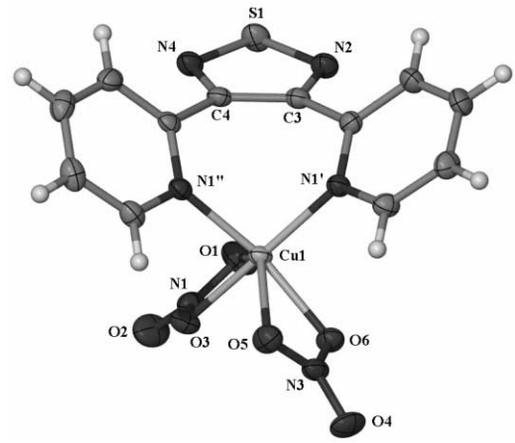

Fig. 3 X-Ray crystal structure of $[Cu(dpt)(NO_3)_2]$, showing perspective view with atom labelling. Selected bond lengths (Å) and angles (°). Cu1–N1′ 2.002(2), Cu1–N1″ 1.979(2), N1′–Cu1–N1″ 93.74(6), Cu1–O5 2.413(2), Cu1–O6 2.014(1), O5–Cu1–O6 58.02(5), O1–Cu1–O3 58.03(6), Cu1–O1 2.373(2), Cu1–O3 2.028(1), S1–N2 1.633(2), S1–N5 1.629(2), N2–C3 1.330(3), C3–C4 1.446(3), C4–N4 1.327(3).

The crystal structure revealed bidentate coordination of the ligand dpt within a seven-membered chelate ring. The dpt ligand coordinates to the copper through the pyridine nitrogens {Cu1–N1′; 2.002(2) Å and Cu1–N1″; 1.979(2)Å}, with a large bite angle {93.74(6)°} at the metal atom. The two nitrate anions are chelating, with one of the coordinating oxygens of each nitrate bonded more strongly than the other, and these complete the pseudo-octahedral coordination of the copper atom. In this structure the conformation of the ligand is remarkably similar to that found in the previously reported copper(II) chloride complex of the *N*-oxide of dpo.[29] The seven-membered chelate ring induces a similar angle between the pyridines {66.3(5)°}, and the copper atom lies below the plane of the thiadiazole ring {1.997(3)Å}.

The results for the palladium and copper complexes with the ligands dpo and dpt indicated that the heterodiazole rings were not participating in coordination, and that, as with the dpo *N*-oxide ligand,[29] the formation of the seven-membered chelate was favoured over a smaller chelate ring size.

A further interest in the investigation of these ligands was their coordination chemistry with silver(I), where there is a significantly different geometric preference for coordination.[30,31] Accordingly, the ligand dpt and $AgNO_3$ were reacted in methanol; the resulting precipitated material was recrystallised from acetonitrile to give colourless crystals, suitable for X-ray analysis. A perspective view of the asymmetric unit is shown in Fig. 4, while the extended structure is shown in Fig. 5.

The complex is a one-dimensional metallopolymer, which crystallises in the monoclinic space group $P2_1/n$. The asymmetric unit contains a silver atom, bonded to a monodentate nitrate anion, and one dpt ligand coordinated to the silver *via* a pyridine nitrogen. The dpt ligand is coordinated to silver atoms through the pyridine nitrogens only, with the thiadiazole ring again not participating in coordination. The ligand acts in a bridging fashion through each of its pyridine nitrogens, separating two silver atoms in the polymeric chain by 7.401(1) Å. The conformation of the ligand can be defined by the angles between each of the mean-planes of the three planar aromatic rings. The two pyridine rings are of a similar pitch relative to the central 1,2,5-thiadiazole ring {45.9(4)° and 31.3(4)°}, but have the nitrogens in the opposite orientation, leading to the metallopolymer having an undulating character. The silver atom is tri-coordinate with the angle between the coordinating nitrogens being 136.54(8)°. The angle at silver between the nitrate anion and N1′ is 81.48(8)°, and this is considerably smaller than the N1″A–Ag1–O13 angle {141.77(8)°}, which

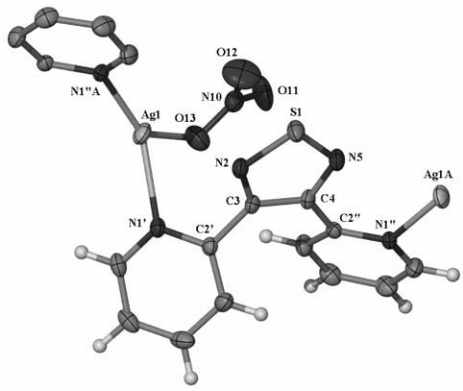

Fig. 4 X-Ray crystal structure of $[Ag(dpt)(NO_3)]_n$, showing perspective view with atom labelling. Selected bond lengths (Å) and angles (°). Ag1–N1′ 2.305(2), Ag1–N1″A 2.235(2), N1′–Ag1–N1″A 136.54(8), Ag1–O13 2.412(3), O13–Ag1–N1′ 81.48(8), S1–N2 1.633(2), S1–N5 1.633(2), N2–S1–N5 98.6(1), N2–C3 1.333(4), S1–N2–C3 107.6(2), C3–C4 1.434(4), N2–C3–C4 113.2(2), C4–N5 1.334(4), C3–C4–N5 112.9(3), C4–N5–S1 107.7(2), C3–C2′ 1.493(4), C4–C2″ 1.478(4).

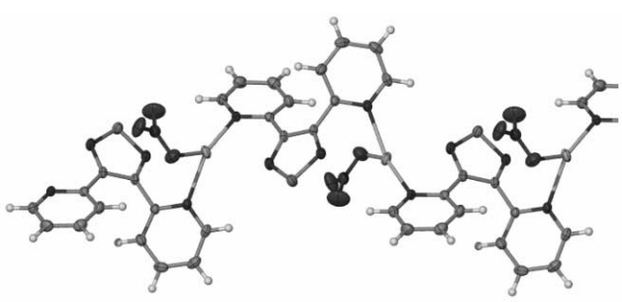

Fig. 5 X-Ray crystal structure of $[Ag(dpt)(NO_3)]_n$, showing perspective of a section of the extended structure.

gives the silver a geometry that is neither trigonal planar nor distorted T-shape.

Dinuclear ruthenium complexes

Homodinuclear complexes of ruthenium with ligands **1** and **2** were also investigated in this study. In ligand-bridged dinuclear complexes containing two octahedral metal centres there exists the possibility of diastereoisomerism between racemic (*rac*; ΛΛ/ΔΔ; point group C_2) and *meso* (ΛΔ; point group C_s) forms.[32]

The dinuclear complex $[(bpy)_2Ru(\mu\text{-dpo})Ru(bpy)_2](PF_6)_4$ (Fig. 6) was prepared by reacting ligand **1** with an excess of

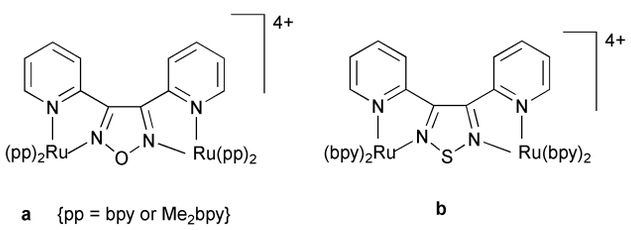

a {pp = bpy or Me_2bpy} b

Fig. 6 Coordination mode of dinuclear complexes involving dpo and dpt as bridging ligands.

$[Ru(bpy)_2Cl_2]$ in refluxing 3 : 1 ethanol–water, and precipitated as the hexafluorophosphate salt. Separation of the diastereoisomeric forms was achieved by cation exchange chromatography using SP-Sephadex C-25 as the support with sodium toluene-4-sulfonate solution as the eluent. Interestingly, the colours of the two diastereoisomeric forms were visually distinguishable on the column and in aqueous solution, with the Band 1 eluant (*rac*) being red while Band 2 (*meso*) was purple. The analogous dpt species $[(bpy)_2Ru(\mu\text{-dpt})Ru(bpy)_2](PF_6)_4$ (Fig. 6b) was synthesised, purified and separated into its diastereoisomeric forms in a similar manner, but using sodium benzoate solution as eluent. The *meso* and *rac* diastereoisomers of $[(bpy)_2Ru(\mu\text{-dpt})Ru(bpy)_2](PF_6)_4$ form in a 3 : 1 ratio. Again, the colours of the two diastereoisomeric forms differed in aqueous solution, with the Band 1 eluant (*rac*) being purple, while Band 2 (*meso*) appeared brown. The $[(Me_2bpy)_2Ru(\mu\text{-dpo})Ru(Me_2bpy)_2](PF_6)_4$ (Fig. 6a; pp = Me_2bpy) was also prepared, but the separation of the diastereoisomers was not undertaken.

The ^1H NMR spectra of the separated diastereoisomers were assigned using a combination of one- and two-dimensional NMR techniques. Noticeable differences exist in the chemical shifts (see Experimental section) of some proton signals in the separate diastereoisomers.

The electrochemical characteristics of the diastereoisomeric forms of $[\{Ru(bpy)_2\}_2(\mu\text{-BL})]^{4+}$ {BL = dpo, dpt} were studied by cyclic and differential pulse voltammetry (Table 1). Examination of the anodic potential region for both complexes revealed two reversible one-electron redox processes corresponding to successive oxidations of the metal centres. Both diastereoisomeric forms of $[\{Ru(bpy)_2\}_2(\mu\text{-dpo})]^{4+}$ revealed a single irreversible reduction process in the cathodic potential region which is assigned to the bridging ligand, while the diastereoisomers of $[\{Ru(bpy)_2\}_2(\mu\text{-dpt})]^{4+}$ exhibited a fully reversible bridging ligand-based reduction process in this region. The large separation between the metal-based redox processes (ΔE_{ox}) in both complexes is indicative of strong electronic communication between the metal centres, with a relatively stronger interaction observed for the diastereoisomers containing the bridging dpo moiety. This indicates a large metal–metal interaction when compared to the dinuclear complexes $[(bpy)_2Ru(\mu\text{-dpp})Ru(bpy)_2]^{4+}$ (ΔE_{ox} = 170 mV)[6,33] and $[(bpy)_2Ru(\mu\text{-dppm})Ru(bpy)_2]^{4+}$ (ΔE_{ox} = 160 mV).[5]

The electrochemistry of $[(bpy)_2Ru(\mu\text{-dpt})Ru(bpy)_2]^{4+}$ became somewhat complicated by adsorption processes at the electrode surface. This has been encountered before in work with sulfur-containing ligands.[33] However, further reduction processes were found in the region between −1130 and −1700 mV, which were assigned to the reductions of the auxiliary bpy ligands.

Significantly, measurable differences were also observed between the electrochemical properties of the diastereoisomeric forms of the same complex, with this difference being most pronounced for the diastereoisomers of $[\{Ru(bpy)_2\}_2(\mu\text{-dpo})]^{4+}$. Indeed, the comproportionation constants (K_c) suggest a significant difference in the stability of the mixed-valence species for the *meso* form of $[(bpy)_2 Ru^{II}(\mu\text{-dpo})Ru^{III}(bpy)_2]^{5+}$ relative to the corresponding *rac* diastereoisomer. Differences in the electrochemical properties of the diastereoisomers of dinuclear ruthenium complexes have been reported previously.[34,35] Spectroelectrochemical investigations on the mixed-valence forms of these complexes are currently in progress in our laboratories in an attempt to explain the origin of this stereochemical dependence of the metal–metal interaction.

The X-ray crystal structures were obtained of the two separated diastereisomeric forms of $[(bpy)_2Ru(\mu\text{-dpo})Ru(bpy)_2]^{4+}$, in each case as the $[ZnCl_4]^{2-}$ salt. The *meso* form (Fig. 7) crystallises in the monoclinic space group $P2_1/n$ with four dinuclear units in the unit cell while the *rac* diastereoisomer (Fig. 8) crystallises in the triclinic space group $P\bar{1}$ with two molecules in the unit cell. Both complexes crystallise as ionic complexes with no significant interactions between the dinuclear cations and the $ZnCl_4^{2-}$ anions. The *meso* isomer crystallises with six molecules of water, while the *rac* isomer co-crystallises with a $[ZnCl_2(H_2O)_2]$ molecule in the lattice. Both cations involve two $[Ru(bpy)_2]^{2+}$ moieties bridged by the 3,4-dipyridyl-1,2,5-oxadiazole (dpo) molecule which acts as a doubly-chelating ligand. Thus each Ru resides in a slightly distorted octahedral environment, with Ru ⋯ Ru separations of 6.016 and 6.014 Å in the *meso* and *rac* isomers respectively. The

Table 1 Redox potentials for the diastereoisomeric forms of $[\{Ru(bpy)_2\}_2(\mu\text{-BL})]^{n+}$ {BL = dpo, dpt}

Complex		$E_{1/2}$ [a,b] E_{red1} [4+/3+]	E_{ox1} [5+/4+]	E_{ox2} [c] [6+/5+]	ΔE_{ox} [c]	10^{-3} K_c [d]
$[\{Ru(bpy)_2\}_2(\mu\text{-dpo})]^{n+}$	Band 1 (*rac*)	−562 [e]	1510	1846	336	478
	Band 2 (*meso*)	−510 [e]	1486	1846	360	1220
$[\{Ru(bpy)_2\}_2(\mu\text{-dpt})]^{n+}$	Band 1 (*rac*)	−658	1421	1679	258	23
	Band 2 (*meso*)	−722	1438	1702	264	29

[a] Potentials quoted in mV *vs.* SCE in CH_3CN–0.1 mol dm^{-3} $[(n\text{-}C_4H_9)_4N]PF_6$ (the ferrocene/ferrocenium couple occurred at +310 mV *vs.* SCE). [b] Uncertainty in $E_{1/2}$ values *ca.* ±5 mV. [c] $\Delta E_{ox} = E_{ox2} - E_{ox1}$. [d] $K_c = \exp\{\Delta E_{ox}F/RT\}$, where F/RT takes the value 38.92 V^{-1} at 298 K.[36] [e] Irreversible reduction (quoted as $E_{p,c}$).

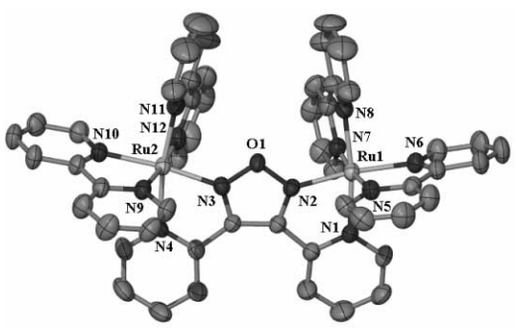

Fig. 7 X-Ray crystal structure of the cation in *meso*-$[(bpy)_2Ru(\mu\text{-dpo})Ru(bpy)_2][ZnCl_4]_2\cdot 6H_2O$. Selected bond lengths (Å): Ru1–N2 1.979(4), Ru1–N6 2.060(4), Ru1–N5 2.068(4), Ru1–N8 2.069(4), Ru1–N7 2.073(4), Ru1–N1 2.079(4), Ru2–N3 1.983(4), Ru2–N12 2.061(5), Ru2–N11 2.062(5), Ru2–N9 2.069(4), Ru2–N10 2.071(4), Ru2–N4 2.085(4). Selected bond angles (°): N2–Ru1–N6 172.90(17), N6–Ru1–N5 78.62(17), N8–Ru1–N7 79.06(18), N2–Ru1–N1 75.67(16), N3–Ru2–N10 173.56(17), N12–Ru2–N11 78.2(2), N9–Ru2–N10 78.52(16), N3–Ru2–N4 75.55(17).

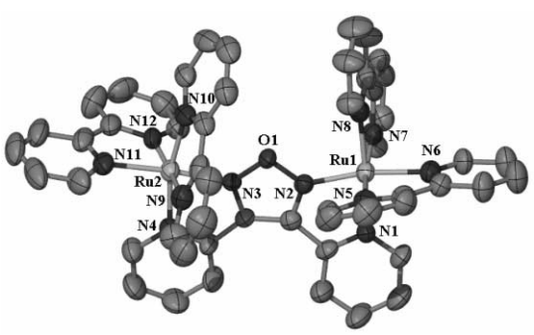

Fig. 8 X-Ray crystal structure of the cation in *rac*-$[(bpy)_2Ru(\mu\text{-dpo})Ru(bpy)_2][ZnCl_4]_2\cdot[ZnCl_2(H_2O)_2]$. Selected bond lengths (Å): Ru1–N2 1.971(7), Ru1–N6 2.046(8), Ru1–N5 2.067(7), Ru1–N8 2.071(7), Ru1–N7 2.062(7), Ru1–N1 2.104(7), Ru2–N3 1.979(7), Ru2–N12 2.046(8), Ru2–N11 2.077(8), Ru2–N9 2.091(8), Ru2–N10 2.081(7), Ru2–N4 2.080(7). Selected bond angles (°): N2–Ru1–N6 170.0(3), N6–Ru1–N5 78.8(3), N8–Ru1–N7 79.6(3), N2–Ru1–N1 75.3(3), N3–Ru2–N11 174.1(3), N12–Ru2–N11 78.8(3), N9–Ru2–N10 9.2(3), N3–Ru2–N4 75.3(3).

dpo ligand is slightly twisted in both complexes with pyridyl–pyridyl interplanar angles of 14.3(3) and 17.1(5)° in the *meso* and *rac* isomers respectively. The interplanar angles between the pyridyl rings and the oxadiazole rings are not as pronounced with deviations of 5.2(3) and 6.3(5)° for the $N(1)_{pyridyl}$ ring and the five-membered ring and 10.2(3) and 13.0(4)° for the $N(4)_{pyridyl}$ ring and the five-membered ring in the *meso* and *rac* isomers respectively. In the structure of the *meso* isomer, all six of the lattice water molecules are involved in hydrogen bonding with two $[ZnCl_4]^{2-}$ anions {both involving Zn(2)}. This hydrogen bonding links the two $[ZnCl_4]^{2-}$ anions *via* a cluster of 12 hydrogen bonded water molecules. The other anion {involving Zn(1)} is a discrete anion with no intermolecular interactions and resides in pockets between adjacent $[(ZnCl_4^{2-})_2(H_2O)_{12}]$ clusters and $[Ru_2(bpy)_4(dpo)]^{4+}$ cations. In the structure of the *rac* isomer there are no such hydrogen bonding interactions. There is however, an unusual tetrahedral $[ZnCl_2(H_2O)_2]$ molecule residing in the lattice. A Cambridge crystallographic database search revealed this molecule has only been crystallographically observed on one occasion, in $[ZnCl_2(H_2O)_2(15\text{-crown-5})]$;[37] typically hydrated zinc salts form $[Zn(H_2O)_6]^{2+}$ ions, but presumably in the present case, there is only limited amount of water in the solvent.

Some of the important factors governing metal–metal interactions are the metal–metal distance, the electron density of the LUMO at the coordinating centres,[38,39] and the nature of the bridge. With short internuclear metal–metal separations, it has been proposed that electron transfer may be through the direct orbital overlap of the metal d orbitals. This point has been particularly made for dinuclear complexes containing a 2,2′-bipyrimidine[38,40] or 2,2′-biimidazolate bridge.[41] In other bridging ligands the geometry is such that direct metal d-orbital overlap is not possible, so that communication must be mediated through the π-system of the bridging ligand, and this is the case with the present examples. The metal–metal interactions of the homodinuclear complexes just described are strong, with ΔE_{ox} = 348 mV {average of *meso* and *rac* diastereoisomers for $[(bpy)_2Ru(\mu\text{-dpo})Ru(bpy)_2]^{4+}$} and ΔE_{ox} = 260 mV {average of *meso* and *rac* diastereoisomers for $[(bpy)_2Ru(\mu\text{-dpt})Ru(bpy)_2]^{4+}$}, which indicate excellent communication of the metals through the bridging ligands. The structural studies (above) indicate an intermetal distance of *ca.* 6.0Å for the dinuclear complex $[(bpy)_2Ru(\mu\text{-dpo})Ru(bpy)_2]^{4+}$ (6.016 Å for *meso*, 6.014 Å for *rac*) which would be similar for the species $[(Me_2bpy)_2Ru(\mu\text{-dpo})Ru(Me_2bpy)_2]^{4+}$ and $[(bpy)_2Ru(\mu\text{-dpt})Ru(bpy)_2]^{4+}$.

As mentioned previously, the ligands dpo (**1**) and dpt (**2**) have a structural similarity to dpp (**3**) and dppm (**4**). However, the replacement of the central diazine rings with a heterodiazole would alter the distance between the metals (more so in the case of dpp), and importantly the electronic nature of the bridge. The degree of aromaticity of the bridge has been postulated to facilitate interaction between the metals. As was mentioned previously, the 1,2,5-oxadiazoles are only 'aromatic' in that they contain six π-electrons, with the oxygen atom contributing little of its electron density into the ring,[27] and thus the heterocyclic 1,2,5-oxadiazole system is perhaps better described as being diene-like. The thiadiazoles may be, because of the greater polarizability of the larger sulfur atom, more delocalised systems. However, this being the case, the low aromatic character of the bridge has not restricted the electronic communication between the metals. In fact, on the basis of the electrochemical results obtained, the low aromatic character has served to enhance the interaction!

Heterodinuclear complexes

We also synthesised some heterodinuclear ruthenium–palladium and ruthenium–platinum complexes incorporating dpo and dpt as the bridging ligand. Similar mixed-metal

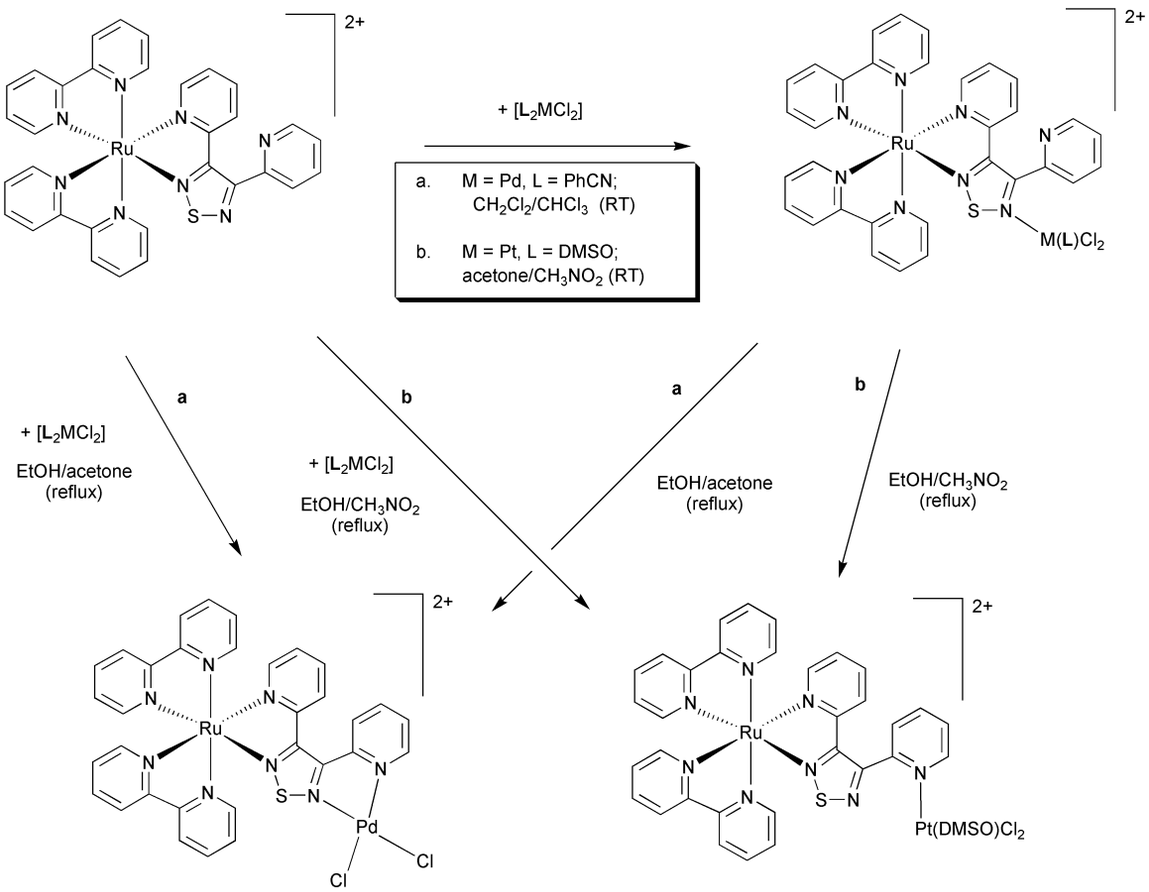

Scheme 3

complexes of dpp have been shown to possess interesting physicochemical properties.[42]

Addition of a methanolic solution of $Li_2[PdCl_4]$ to the complex $[Ru(bpy)_2(dpt)]^{2+}$ dissolved in hot acetone–ethanol resulted in an immediate precipitate identified by FABMS as the chloride salt, $[(bpy)_2Ru(\mu\text{-}dpt)PdCl_2]Cl_2$. The appearance and position (9.35 ppm) of a pyridine H6 proton (H6′) in the ^1H NMR spectrum (CD_3CN solvent) readily distinguished the pyridine ring of the thiadiazole-containing ligand coordinated to palladium. The chemical shifts of the other protons of this ring were found by 1-D TOCSY from the irradiation of this signal. The related complex, $[(Me_2bpy)_2Ru(\mu\text{-}dpo)PdCl_2]Cl_2$, was also prepared, and showed similar coordination induced shifts of the pyridine ring coordinated to palladium.

In order to perform electrochemical measurements the chloride anion needed to be exchanged for a non-redox active counter ion. When the normal metathesis techniques proved unsuccessful, an alternative route was sought. An equimolar quantity of bis(benzonitrile)dichloropalladium $[(PhCN)_2PdCl_2]$ in chloroform was added to the mononuclear ruthenium complex $[Ru(bpy)_2(dpt)](PF_6)_2$ dissolved in dichloromethane at room temperature, which resulted in a product obtained in high yield. FAB-MS of the resulting solid gave a molecular ion that suggested the complex contained a $PdCl_2$ fragment as well as a coordinated benzonitrile and so was formulated as $[(bpy)_2Ru(\mu\text{-}dpt)Pd(PhCN)Cl_2](PF_6)_2$. A ^1H NMR spectrum in deuterated acetonitrile showed that the product had some very similar chemical shifts compared to the precursor ruthenium complex. Therefore the resulting complex was proposed as the alternative dinuclear species shown in Scheme 3, where the palladium has coordinated to the N5 of the thiadiazole in a monodentate fashion.

When the reaction conditions were changed to refluxing in acetone–ethanol, the desired chelated complex, $[(bpy)_2Ru(\mu\text{-}dpt)PdCl_2](PF_6)_2$, was formed. Also, the complex $[(bpy)_2Ru(\mu\text{-}dpt)Pd(PhCN)Cl_2](PF_6)_2$ could be converted to the $[(bpy)_2Ru(\mu\text{-}dpt)PdCl_2](PF_6)_2$ by the same conditions (Scheme 3a; M = Pd, L = PhCN).

A ruthenium–platinum complex was prepared by reacting equimolar amounts of the mononuclear ruthenium complex $[Ru(bpy)_2(dpt)]^{2+}$ with $[(DMSO)_2PtCl_2]$ in acetone–nitromethane at room temperature (Scheme 3b; M = Pt, L = DMSO). Careful inspection of the ^1H NMR spectrum revealed that the complex formed contained an uncoordinated pyridine ring of the ligand. In an analogous manner to the Ru–Pd dinuclear species described above, the metal fragment appeared to be coordinated to the thiadiazole N5 in a monodentate fashion. The complex was then heated at reflux in ethanol–nitromethane, in the hope of converting it to the desired chelating complex. However, FAB-MS again indicated the presence of coordinated DMSO. Accordingly, the complex was formulated as $[(bpy)_2Ru(\mu\text{-}dpt)PtCl_2(DMSO)](PF_6)_2$. The H6 proton of the pyridyl ring coordinated to the platinum was identified in the spectrum by its appearance and downfield position (9.07 ppm). This proton had changed in chemical shift and suggested another mode of coordination. Irradiation of this signal gave the chemical shifts of the other protons of the ring. Changes in the chemical shifts of the protons of this ring, in particular H4′, suggested that the platinum fragment was now coordinated to the pyridine ring. In general, considerable overlap of the signals for the bpy ligands in the ^1H NMR spectrum was observed, and no attempts to assign any of the individual bpy ring systems were made.

Conclusion

In this study we have prepared the first examples of chelating ligands containing 1,2,5-oxadiazole and 1,2,5-thiadiazole

subunits. The ligands **1** and **2** exhibit a variety of modes of coordination with different metals. Studies of their ruthenium complexes show that these ligands have very low energy LUMOs and, most importantly, that they facilitate unusually strong metal–metal interactions across the heterodiazole bridge, the magnitude of which depends on the specific diastereoisomer.

Experimental

Physical measurements

^{1}H NMR experiments were performed on a Varian Mercury or Unity 300 MHz NMR spectrometer at room temperature. ^{1}H NMR assignments were made with the assistance of COSY and/or TOCSY experiments to identify each pyridine ring spin system, while individual protons within a ring were assigned on the basis of their chemical shifts and the following typical ^3J coupling patterns for pyridine protons: H3 (d, J = 8 Hz), H4 (t, J = 8 Hz), H5 (dd, J = 8, 5 Hz), H6 (d, J = 5 Hz). ^{13}C NMR experiments were performed on a Varian Unity 300 MHz NMR spectrometer. Mass spectra (EI and FAB) were recorded using a Kratos MS80RFA mass spectrometer with a Mach 3 data system. Electron Impact (EI) spectra were obtained at 70 eV with a source temperature of 250 °C. Fast Atom Bombardment (FAB) spectra were acquired in a nitrobenzyl alcohol matrix using an Iontech ZN11NF FAB gun operated at 8 KV and 2 mA. Electrospray (ES) mass spectra were recorded using a Micromass LCT TOF mass spectrometer, with a probe operating at 3200 V and cone voltage of 30 V. Samples were dissolved in 1 : 1 acetonitrile–water, and spectra acquired using source and desolvation temperatures of 80 °C and 150 °C, respectively. Elemental analyses were performed by the Campbell Microanalytical Laboratory at the University of Otago.

Electrochemical measurements were performed under argon using a Bioanalytical Systems BAS 100A Electrochemical Analyser. Cyclic and differential pulse voltammograms were recorded in acetonitrile-0.1 mol dm^{-3} [(n-C_4H_9)$_4$N]PF_6 solution using a glassy carbon or platinum button working electrode, a platinum wire auxiliary electrode and an Ag/AgCl (0.1 mol dm^{-3} [(n-C_4H_9)$_4$N]PF_6 in acetonitrile) reference electrode. Ferrocene was added as an internal standard on completion of each experiment (the ferrocene/ferrocenium couple occurred at +550 mV *vs.* Ag/AgCl). All values are quoted *vs.* SCE. Cyclic voltammetry was performed with a sweep rate of 100 mV s^{-1}; differential pulse voltammetry was conducted with a sweep rate of 4 mV s^{-1} and a pulse amplitude, width and period of 50 mV, 60 ms and 1 s, respectively.

Materials

$RuCl_3 \cdot xH_2O$ (Strem, 99%), palladium chloride (BDH, 99%), silver nitrate (Aldrich, 99+%), 2,2′-bipyridine (bpy; Aldrich, 99+%), stannous chloride (Ajax), ammonium hexafluorophosphate (NH_4PF_6; Aldrich, 99.99%), potassium hexafluorophosphate (KPF_6; Aldrich, 98%), tetra-*n*-butylammonium hexafluorophosphate ([(n-C_4H_9)$_4$N]PF_6; Fluka, 99+%), hydroxylamine hydrochloride (Aldrich, 99%), zinc chloride ($ZnCl_2 \cdot 2H_2O$; Fluka, 98%), sodium toluene-4-sulfonate (Aldrich, 98%), sodium benzoate (Aldrich, 98%), and laboratory reagent solvents were used as received. Trithiazyl trichloride,[43,44] 1,2-di(2-pyridyl)ethene,[25] $[Ru(bpy)_2Cl_2] \cdot 2H_2O$,[45] $[Ru(Me_2bpy)_2Cl_2] \cdot 2H_2O$,[46] $[Ru(DMSO)_4Cl_2]$,[47] $[(PhCN)_2PdCl_2]$,[48] and $[(DMSO)_2PtCl_2]$[49] were prepared according to literature procedures. Acetonitrile (Aldrich, 99.9+%) was distilled under nitrogen from CaH_2 immediately prior to use. SP Sephadex C-25 (Amersham Pharmacia Biotech) and silica gel 200–400 mesh (Aldrich) were employed for the chromatographic separation and purification, respectively, of ruthenium complexes.

Ligand syntheses

3,4-Di(2-pyridyl)-1,2,5-oxadiazole (1; dpo). 2,2′-Pyridil (4.03 g, 19.0 mmol), hydroxylammonium chloride (5.19 g, 74.6 mmol) and NaOH (16 g) were combined in a 250 ml round bottom flask with a magnetic stirring bar. H_2O (80 ml) was added and the solution stirred for 40 h. The solution was cooled in an ice-bath and conc. HCl was added dropwise until a flocculent precipitate developed. The solid was collected by filtration and washed with a small amount of cold water. Mp 243–244 °C; yield 2.39 g (52%). Positive-ion EI-MS: Calc. m/z for $C_{12}H_{10}N_4O_2$ 240.0647; found 240.0633; m/z 240.0 (M^+, 2.61%), 224.0 ($M^+ - H_2O$, 61%), 207.1 ($M^+ - 2H_2O$, 87%), 104.0 ($PyCN^+$, 100%), 78.0 (Py^+, 62%). ^{1}H NMR (d$_6$-DMSO) δ: 7.35, H5′; 7.49, H3′; 7.85, H4′; 8.60, H6′; 11.72, N–O*H*. ^{13}C NMR (d$_6$-DMSO) δ: 124.77, C5′; 126.26, C3′; 136.15, C4′; 149.14, C6′; 152.04, C1/C2; 154.56, C2′.

The above dioxime (2.01 g, 8.3 mmol) and H_2O (2 ml) were placed in a tube (dimensions 33 mm ID × 41 mm OD; vol. 85 ml) and the tube sealed, placed in an oven and heated at 185 °C for 18 h. The tube was then allowed to come to room temperature and the contents rinsed out with methanol. The washings were collected and the solvent removed *in vacuo* to give a red solid residue. Chromatography on silica gel (30 g, elution with 3 : 1 petroleum ether : ethyl acetate) successfully separated dpo, which was then recrystallised from 3 : 1 petroleum ether–ethyl acetate. Mp 122–123 °C; yield 0.82 g (44%). (Found: C, 64.1; H, 3.29; N, 25.1. Calc. for $C_{12}H_8N_4O$: C, 64.3; H, 3.60; N, 25.0). Positive-ion EI-MS: Calc. m/z for $C_{12}H_8N_4O$ 224.0698; found 224.0701. m/z 224.1 (M^+, 23%), 104.0 ($PyCN^+$, 21%), 78.0 (Py^+, 100%). ^{1}H NMR ($CDCl_3$) δ: 7.40, H5′; 7.84, H4′; 7.92, H3′; 8.60, H6′. ^{13}C NMR ($CDCl_3$) δ: 124.74/124.67, C3′/C5′; 136.76, C4′; 146.23, C2′; 149.69, C6′; 153.34, C3/C4.

3,4-Di(2-pyridyl)-1,2,5-thiadiazole (2; dpt). 1,2-Di(2-pyridyl)-ethene (0.59 g, 3.3 mmol) was dissolved in a mixture of dry toluene (5 ml) and dry pyridine (2 ml). Trithiazyl trichloride ($S_3N_3Cl_3$; 0.83 g, 3.4 mmol) dissolved in dry toluene (15 ml) was added dropwise with stirring at room temperature. The clear solution became green and a precipitate developed. The mixture was set to reflux with stirring for 18 h, giving a clear red solution with a small amount of brown precipitate. After cooling, the solution was decanted into a separating funnel and more toluene (20 ml) added. The solution was washed with saturated aqueous $NaHCO_3$ (3 × 20 ml), then with H_2O (1 × 20 ml). To the solid precipitate was added H_2O (*ca.* 30 ml), then solid $NaHCO_3$ with swirling until pH 8. This solution was then extracted with toluene (3 × 10 ml). The organic fractions were combined, dried (anhydrous Na_2SO_4), then the solvent removed *in vacuo*. Chromatography on silica gel (2 × 30 cm) with ethyl acetate as the eluent separated dpt (R_f 0.61), which was recrystallised from ethanol–water. Mp 63–69 °C; yield 0.39 g (49%). (Found: C, 60.2; H, 3.38; N, 23.1; S, 13.1. Calc. for $C_{12}H_8N_4S$: C, 60.0; H, 3.36; N, 23.3; S, 13.3). Positive-ion EI-MS: Calc. m/z for $C_{12}H_8N_4S$ 240.0470; found 240.0391. ^{1}H NMR ($CDCl_3$) δ: 7.30, H5′; 7.78, H3′; 7.78, H4′; 8.50, H6′. ^{13}C NMR ($CDCl_3$) δ: 123.73, C5′; 124.20, C3′; 136.45, C4′; 149.11, C6′.

Complex syntheses and diastereoisomer separation

Bis(2,2′-bipyridine)(N2,N1′-[3,4-di(2-pyridyl)-1,2,5-oxadiazolyl])ruthenium(II) hexafluorophosphate, $[Ru(bpy)_2(dpo)](PF_6)_2$. The ligand dpo (15.0 mg, 0.067 mmol) and $[Ru(bpy)_2Cl_2] \cdot 2H_2O$ (34.8 mg, 0.067 mmol) in 3 : 1 EtOH–H_2O (8 ml) were refluxed for 4 h. After cooling, the reaction mixture was concentrated to dryness *in vacuo*. The residue was re-dissolved in the minimum of water, filtered to remove unreacted ligand, and the product precipitated by the addition of an aqueous solution of NH_4PF_6. Yield 56.0 mg (92%). (Found: C, 41.5; H, 2.48; N, 12.1. Calc. for $C_{32}H_{24}N_8F_{12}OP_2Ru$: C, 41.4; H, 2.61; N, 12.1). Positive-ion

FAB-MS: Calc. *m*/*z* for $C_{32}H_{24}N_8F_6OPRu^+$ {[(bpy)$_2$Ru(dpo)](PF$_6$)$^+$} 783.0773; found 783.0758. Visible spectrum: λ_{max} (CH_3CN) 435 nm, ε 13 400 M^{-1} cm^{-1}. Electrochemistry (cyclic voltammetry; CH_3CN): $E_{1/2}$ (Ru^{2+}/Ru^{3+}) = 1510 mV; for reduction, $E_{p,c}$ = −970 mV (irreversible). ^{1}H NMR (CD_3CN) δ: 7.50, H5b; 7.53, H5a; 7.54, H5c; 7.57, H5d; 7.59, H5-dpo; 7.74, H6c; 7.77, H5′-dpo; 7.79, H6d; 7.86, H6b; 7.88, H6-dpo; 8.03, H6a; 8.16, H5′-dpo; 8.16, H4c; 8.17, H4b; 8.18, H4a; 8.22, H4-dpo; 8.23, H4d; 8.27, H3′-dpo; 8.56, H3b; 8.58, H3c; 8.59, H3a; 8.63, H3d; 9.03, H6′-dpo; 9.86, H3-dpo.

Bis(4,4′-dimethyl-2,2′-bipyridine)(N2,N1′-[3,4-di(2-pyridyl)-1,2,5-oxadiazolyl])ruthenium(II) hexafluorophosphate, [Ru(Me$_2$bpy)$_2$(dpo)](PF$_6$)$_2$. Ligand dpo (10.0 mg, 0.045 mmol) and [Ru(Me$_2$bpy)$_2$Cl$_2$]·2H$_2$O (25.8 mg, 0.045 mmol) in 3 : 1 EtOH–H$_2$O (8 ml) were refluxed for 4 h. After cooling, the reaction mixture was concentrated to dryness *in vacuo*. The residue was re-dissolved in the minimum of water, filtered to remove unreacted ligand and the product precipitated out by the addition of an aqueous solution of NH_4PF_6. Yield 19.1 mg (89%). (Found: C, 43.8; H, 3.41; N, 11.1. Calc. for $C_{36}H_{32}N_8F_{12}OP_2Ru$: C, 44.0; H, 3.28; N, 11.4). Positive-ion FAB-MS: Calc. *m*/*z* for $C_{32}H_{24}N_8F_6OPRu^+$ {[(Me$_2$bpy)$_2$Ru(dpo)](PF$_6$)$^+$} 778.0910; found 778.0891. Visible spectrum: λ_{max} (CH_3CN) 441 nm, ε 23 500 M^{-1} cm^{-1}. Electrochemistry (cyclic voltammetry; CH_3CN): $E_{1/2}$ (Ru^{2+}/Ru^{3+}) = 1400 mV; for reduction, $E_{p,c}$ = −1080 mV (irreversible). ^{1}H NMR (CD_3CN) δ: 2.60, CH_3; 2.62, 2 × CH_3; 2.64, CH_3; 7.35, 3 × H5; 7.40, H5; 7.52, H6; 7.56, H5-dpo; 7.59, H6; 7.67, H6; 7.76, H5′-dpo; 7.82, H6; 7.85, H6-dpo; 8.17, H5-dpo; 8.18, H5′-dpo; 8.25, H3′-dpo; 8.42, H3; 8.43, 2 × H3; 8.48, H3; 9.02, H6′-dpo; 9.80, H3-dpo.

Bis(2,2′-bipyridine)(N2,N1′-[3,4-di(2-pyridyl)-1,2,5-thiadiazolyl])ruthenium(II) hexafluorophosphate, [Ru(bpy)$_2$(dpt)](PF$_6$)$_2$. Ligand dpt (45 mg, 0.19 mmol) and [Ru(bpy)$_2$Cl$_2$]·2H$_2$O (105 mg, 0.20 mmol) in 3 : 1 EtOH–H$_2$O (8 ml) were refluxed for 5 h. After cooling, the reaction mixture was concentrated to dryness *in vacuo*. The residue was re-dissolved in the minimum of water, filtered to remove unreacted ligand, and the product precipitated out by the addition of an aqueous solution of NH_4PF_6. Chromatography on alumina (7 g, elution with 50 : 1 dichloromethane–methanol) separated the desired mononuclear complex. Yield 153 mg (87%). (Found: C, 40.5; H, 2.46; N, 11.6. Calc. for $C_{32}H_{24}N_8F_{12}P_2RuS$: C, 40.7; H, 2.56; N, 11.9). Positive-ion FAB-MS: Calc. *m*/*z* for $C_{32}H_{24}N_8F_6PRuS^+$ {[(bpy)$_2$Ru(μ-dpt)](PF$_6$)$^+$} 759.0540; found 759.0537. Visible spectrum: λ_{max} (CH_3CN) 454 nm, ε 15 000 M^{-1} cm^{-1}. Electrochemistry (cyclic voltammetry; CH_3CN): $E_{1/2}$ (Ru^{2+}/Ru^{3+}) = 1370 mV; for reduction, $E_{p,c}$ = −1180, −1530 mV (irreversible). ^{1}H NMR (CD_3CN) δ: 7.49, H5-dpt; 7.50, H5a; 7.51, H5b; 7.52, H5c; 7.52, H5d; 7.74, H5′-dpt; 7.77, H6d; 7.81, H6c; 7.86, H6-dpt; 7.88, H6a; 7.92, H6b; 8.03, H4-dpt; 8.09, H3′-dpt; 8.12, H5′-dpt; 8.16, H4b; 8.18, H4c; 8.18, H4d; 8.20, H4a; 8.59, H3b; 8.59, H3d; 8.60, H3a; 8.61, H3c; 8.90, H6′-dpt; 9.02, H3-dpt.

Tris(N2,N1′-[3,4-di(2-pyridyl)-1,2,5-thiadiazolyl])ruthenium(II) hexafluorophosphate, [Ru(dpt)$_3$](PF$_6$)$_2$. The ligand dpt (105.6 mg, 0.44 mmol) and [Ru(DMSO)$_4$Cl$_2$] (63.0 mg, 0.13 mmol) in 3 : 1 ethanol–water (8 ml) were refluxed for 24 h. After cooling, the reaction mixture was concentrated to dryness *in vacuo*. The residue was re-dissolved in the minimum of water, filtered to remove unreacted ligand, and the product precipitated out by the addition of an aqueous solution of NH_4PF_6 and purified by chromatography on alumina (1 × 5 cm) with 200 : 1 dichloromethane–methanol as eluent. Yield 113 mg (78%). (Found: C, 38.4; H, 2.36; N, 14.6; S, 8.6. Calc. for $C_{36}H_{24}N_{12}F_{12}P_2RuS_3\cdot H_2O$: C, 38.3; H, 2.32; N, 14.9; S, 8.5). Visible spectrum: λ_{max} (CH_3CN) 435 nm, ε 18 900 M^{-1} cm^{-1}. Electrochemistry (cyclic voltammetry; CH_3CN): $E_{p,c}$ (for reduction) = −730 mV (irreversible).

Tris(N2,N1′-[3,4-di(2-pyridyl)-1,2,5-oxadiazolyl])ruthenium(II) hexafluorophosphate, [Ru(dpo)$_3$](PF$_6$)$_2$. The ligand dpo (31.6 mg, 0.14 mmol) and [Ru(DMSO)$_4$Cl$_2$] (19.5 mg, 0.04 mmol) in 3 : 1 ethanol–water (6 ml) were refluxed for 5 h. After cooling, the reaction mixture was concentrated to dryness *in vacuo*. The residue was re-dissolved in the minimum of water, filtered to remove unreacted ligand, and the product precipitated out by the addition of an aqueous solution of NH_4PF_6 and purified by chromatography on alumina (1 × 4 cm) with 200 : 1 dichloromethane–methanol as eluent. Yield 19 mg (45%). Positive-ion FAB-MS: Calc. *m*/*z* for $C_{36}H_{24}N_{12}F_6O_3PRu^+$ {[Ru(dpo)$_3$](PF$_6$)$^+$} 919.0810; found 919.0780. Visible spectrum: λ_{max} (CH_3CN) 401 nm, ε 16 900 M^{-1} cm^{-1}. Electrochemistry (cyclic voltammetry; CH_3CN): $E_{p,c}$ (for reduction) = −410 mV (irreversible).

[N1′,N1″-3,4-Di(2-pyridyl)-1,2,5-oxadiazolyl]dichloropalladium(II), [Pd(dpo)Cl$_2$]. An excess of 0.0904M $Li_2[PdCl_4]$ solution was added to ligand dpo (6.5 mg, 0.029 mmol) dissolved in methanol (1 ml). The fine yellow precipitate that developed was collected by filtration. Mp >300 °C; yield 11.1 mg (95%). (Found: C, 35.7; H, 2.04; N, 13.4; Cl, 17.4. Calc. for $C_{12}H_8N_4Cl_2OPd$: C, 35.9; H, 2.01; N, 14.0; Cl, 17.7). ^{1}H NMR (d$_6$-DMSO) δ: 8.05, H3; 8.26, H4; 7.86, H5; 9.15, H6.

[N1,N1″-3,4-Di(2-pyridyl)-1,2,5-thiadiazolyl]dichloropalladium(II), [Pd(dpt)Cl$_2$]. An excess of 0.0904M $Li_2[PdCl_4]$ was added to the ligand dpt (19.4 mg, 0.081 mmol) dissolved in methanol (2 ml). The yellow precipitate that formed was collected by filtration and washed with methanol. Mp >300 °C; yield 30.3 mg (90%). (Found: C, 34.5; H, 2.02; N, 13.0; S, 7.7. Calc. for $C_{12}H_8N_4Cl_2PdS$: C, 34.5; H, 1.93; N, 13.4; S, 7.7). ^{1}H NMR (d$_6$-DMSO) δ: 8.93, H3; 8.19, H4; 7.79, H5; 9.08, H6.

[3,4-Di(2-pyridyl)-1,2,5-thiadiazolyl]dichloroplatinum(II), [Pt(dpt)Cl$_2$]. The ligand dpt (37.5 mg, 0.155 mmol) dissolved in nitromethane (2 ml) was added to [(DMSO)$_2$PtCl$_2$] (66.5 mg, 0.158 mmol) dissolved in nitromethane (3 ml), and the clear solution left overnight after which the resulting yellow microcrystals were filtered off. Mp >300 °C; yield 71.2 mg (91%). (Found: C, 28.5; H, 1.67; N, 10.8; Cl, 13.9; S, 6.1. Calc. for $C_{12}H_8N_4Cl_2PtS$: C, 28.5; H, 1.60; N, 10.8; Cl, 14.0; S, 6.2). ES-MS: Calc. for $C_{12}H_8N_4ClPtS^+$: 469.9806; found 469.9788.

[N1,N1″-3,4-Di(2-pyridyl)-1,2,5-thiadiazolyl]dinitratocopper(II), [Cu(dpt)(NO$_3$)$_2$]. The ligand dpt (39.5 mg, 0.160 mmol) dissolved in methanol (2.5 ml) was added to $Cu(NO_3)_2\cdot 3H_2O$ (85.0 mg, 0.350 mmol) dissolved in methanol (2.5 ml). After several days the sky blue crystals that had formed were collected by filtration. Mp 190–200 °C; yield 41.1 mg (58%). (Found: C, 33.8; H, 1.84; N, 19.3. Calc. for $C_{12}H_8N_6O_6CuS$: C, 33.7; H, 1.88; N, 19.6).

[N1,N1″-3,4-di(2-pyridyl)-1,2,5-thiadiazole(nitrato)silver(I)]$_n$. $AgNO_3$ (26.3 mg 0.154 mmol) dissolved in hot methanol (2.5 ml) was added to the ligand dpt (37.9 mg, 0.158 mmol) dissolved in methanol (3 ml). After several days a powder had formed, and the methanolic solution was withdrawn. The remaining solid was recrystallised from acetonitrile. Yield 56 mg (88%). (Found: C, 35.2; H, 1.85; N, 17.2. Calc. for $C_{12}H_8N_4O_3AgS$: C, 35.1; H, 1.97; N, 17.1).

Bis[bis(4,4′-dimethyl-2,2′-bipyridine)ruthenium(II)]-(μ-[3,4-di(2-pyridyl)-1,2,5-oxadiazolyl]) hexafluorophosphate, [(Me$_2$bpy)$_2$Ru(μ-dpo)Ru(Me$_2$bpy)$_2$](PF$_6$)$_4$. The ligand dpo (15.5 mg, 0.069 mmol) and [Ru(Me$_2$bpy)$_2$Cl$_2$]·2H$_2$O (80 mg, 0.138 mmol) in 3 : 1 EtOH–H$_2$O (16 ml) were refluxed for 24 h. After cooling,

the reaction mixture was concentrated to dryness *in vacuo*. The residue was re-dissolved in the minimum of water, filtered to remove unreacted ligand, and the product precipitated out by the addition of an aqueous solution of NH_4BF_4. Additional product was obtained by extraction of the aqueous solution with dichloromethane. Chromatography on alumina separated the mononuclear complex from the dinuclear complex. The ^{1}H NMR spectrum of $[(Me_2bpy)_2Ru(\mu\text{-dpo})Ru(Me_2bpy)_2](PF_6)_4$ showed the presence of two diastereoisomers in a ratio of 5 : 6. The isomers were not assigned to the *meso* or the *rac* forms. Yield 42 mg (35%). Positive-ion FAB-MS: Calc. *m/z* for $C_{60}H_{56}N_{12}F_{18}OP_3Ru_2^+$ $\{[(Me_2bpy)_2Ru(\mu\text{-dpo})Ru(Me_2bpy)_2](PF_6)_3^+\}$ 1599.1727; found 1599.1713. Visible spectrum: λ_{max} (CH_3CN) 497 nm, ε 15,000 M^{-1} cm^{-1}. Electrochemistry (cyclic voltammetry; CH_3CN): $E_{1/2}$ = 1420, 1800 mV; for reduction, $E_{p,c}$ = −580 mV (irreversible). ^{1}H NMR (CD_3CN) δ: 2.54, 2 × CH_3; 2.56, 2 × CH_3; 2.57, 2 × CH_3; 2.61, 2 × CH_3; 2.62, 4 × CH_3; 2.64, 2 × CH_3; 2.71, 2 × CH_3; 6.96, 4 × H5′; 7.14, 6 × H5′; 7.26, 2 × H6; 7.30, 2 × H6; 7.42, 2 × H5; 7.45, 4 × H6′; 7.53, 4 × H6/H5; 7.66, 4 × H5′-dpo; 7.73, 2 × H6; 7.90, 2 × H6-dpo; 7.98, 2 × H6-dpo; 8.04, 2 × H6; 8.19, 2 × H3; 8.22, 2 × H3; 8.24, 2 × H3; 8.33, 4 × H4′-dpo; 8.39, 4 × H3′; 8.44, 4 × H3′; 8.47, 4 × H3′; 8.96, 4 × H3′-dpo {refer to Fig. 9 for numbering system}.

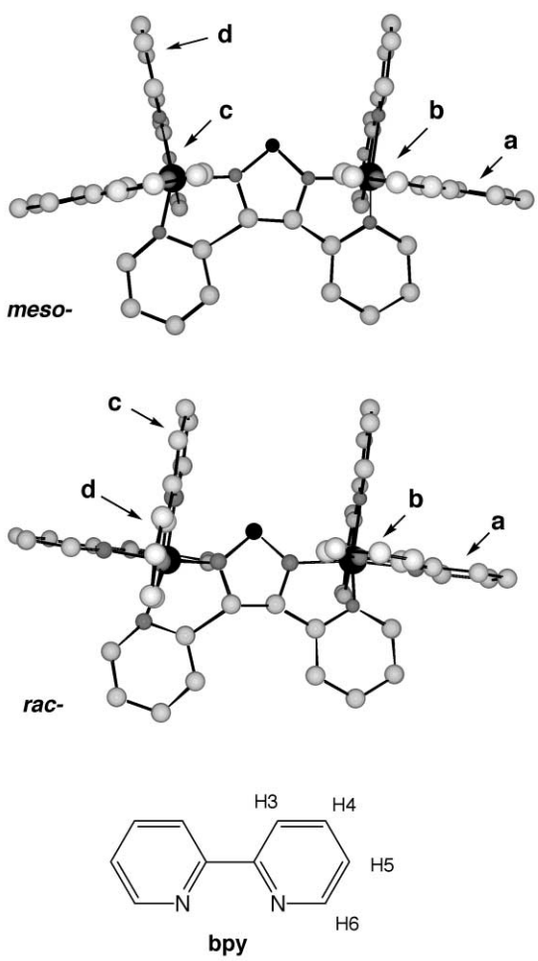

Fig. 9 Numbering system used in reporting NMR spectra of $[(pp)_2Ru(\mu\text{-BL})Ru(pp)_2]^{4+}$ complexes {BL = dpo, dpt; pp = bpy, Me_2bpy}.

Bis[bis(2,2′-bipyridine)ruthenium(II)]-(μ-[3,4-di(2-pyridyl)-1,2,5-oxadiazolyl]) hexafluorophosphate, $[(bpy)_2Ru(\mu\text{-dpo})Ru(bpy)_2](PF_6)_4$. The ligand dpo (36.6 mg, 0.163 mmol) was refluxed with $[Ru(bpy)_2Cl_2]\cdot 2H_2O$ (187 mg, 0.359 mmol) in 3 : 1 ethanol–water (20 cm^3) for 24 h under nitrogen. Ethanol was removed *via* rotary evaporation and the crude product precipitated from the aqueous solution by addition of a saturated solution of KPF_6. A dark red solid was isolated by vacuum filtration and washed with diethyl ether. Purification was achieved by cation exchange chromatography (SP Sephadex C-25; eluent 0.5 mol dm^{-3} NaCl). An orange band of mononuclear material eluted first, followed by the desired dark red product, which was isolated as both BF_4^- and PF_6^- salts. Yield: 130 mg (49%). (Found: C, 44.1; H, 2.94; N, 11.9. Calc. for $C_{52}H_{40}N_{12}B_4F_{16}ORu_2\cdot H_2O$: C, 44.1; H, 2.99; N, 11.9). Positive-ion FAB-MS: Calc. *m/z* for $C_{52}H_{40}N_{12}F_{12}OB_3Ru_2^+$ ($[(bpy)_2Ru(\mu\text{-dpo})Ru(bpy)_2](BF_4)_3^+$) 1312.1631; found 1312.1635.

Separation of the diastereoisomers was achieved by cation exchange chromatography on SP Sephadex C-25 support using 0.20 mol dm^{-1} sodium toluene-4-sulfonate solution as the eluent.[50] The diastereoisomers separated after passing through an effective column length of 180 cm. The two bands were collected and precipitated as the PF_6^- salts by addition of a saturated solution of KPF_6. Rigorous purification methods were employed prior to characterisation due to the potentially strong associations between the complex cations and the anions present in the eluents employed for the chromatographic separations.[50,51] Each product was dissolved in a minimum volume of acetone and loaded onto a short column of silica gel, washed with acetone, water and acetone and then eluted with acetone containing 5% NH_4PF_6. Addition of water and removal of the acetone under reduced pressure afforded a product suitably pure for the physical measurements.

Bands 1 (red) and 2 (purple) were determined to be the *rac* and *meso* diastereoisomers, respectively, as established by X-ray crystallography and NMR characterisation. Diastereoisomeric ratio (*meso* : *rac*) = 6:5. **Band 1**; *rac*. Visible spectrum: λ_{max} (CH_3CN) 496 nm, ε 11 910 M^{-1} cm^{-1}; 406 nm, ε 19 500 M^{-1} cm^{-1}. Electrochemistry (CH_3CN): $E_{1/2}$ = 1510, 1846 mV; for reduction, $E_{p,c}$ = −562 mV (1e$^-$, irreversible), $E_{1/2}$ = −1582 (2e$^-$), −1834 (1e$^-$), −2281 mV (1e$^-$). ^{1}H NMR (CD_3CN) δ: 7.09, H6b; 7.11, H5b; 7.23, H5d; 7.37, H6d; 7.51, H5c; 7.62, H5a/H5-dpo; 7.71, H6c; 7.88, H6-dpo; 7.91, H6a; 7.95, H4d; 8.05, H4b; 8.16, H4c; 8.25, H4a; 8.26, H3d; 8.27, H4-dpo; 8.44, H3a; 8.46, H3b; 8.53, H3c; 8.86, H3-dpo. **Band 2**; *meso*. Visible spectrum: λ_{max} (CH_3CN) 498 nm, ε 11 150 M^{-1} cm^{-1}; 405 nm, ε 19 770 M^{-1} cm^{-1}. Electrochemistry (CH_3CN): $E_{1/2}$ = 1486, 1846 mV; for reduction, $E_{p,c}$ = −510 mV (1e$^-$, irreversible), $E_{1/2}$ = −1511 (1e$^-$), −1570 (1e$^-$), −1790 (1e$^-$), −2226 mV (1e$^-$). ^{1}H NMR (CD_3CN) δ: 7.19, H5d; 7.23, H5b; 7.42, H6b; 7.45, H5c; 7.52, H6d; 7.53, H5a; 7.59; H5-dpo; 7.62, H6c; 7.83, H6-dpo; 7.98, H4d; 8.02, H4b; 8.16, H4a/H4c; 8.19, H6a; 8.27, H4-dpo; 8.31, H3d; 8.34, H3b; 8.52, H3c; 8.56, H3a; 8.87, H3-dpo {refer to Fig. 9 for numbering system}.

Bis[bis(2,2′-bipyridine)ruthenium(II)]-(μ-[3,4-di(2-pyridyl)-1,2,5-thiadiazolyl]) hexafluorophosphate, $[(bpy)_2Ru(\mu\text{-dpt})Ru(bpy)_2](PF_6)_4$. The ligand dpt (30 mg, 0.125 mmol) and $[Ru(bpy)_2Cl_2]\cdot 2H_2O$ (130 mg, 0.250 mmol) in 3 : 1 EtOH–H_2O (16 ml) were refluxed for 24 h. After cooling, the reaction mixture was concentrated to dryness *in vacuo*. The residue was re-dissolved in the minimum of water, filtered to remove unreacted ligand, and the product precipitated out by the addition of an aqueous solution of NH_4PF_6. Chromatography on alumina separated the mononuclear complex (elution with 50 : 1 dichloromethane–methanol) from the dinuclear complex (elution with acetonitrile). Yield 97 mg (47%) (Found: C, 37.6; H, 2.35; N, 10.1. Calc. for $C_{52}H_{40}N_{12}F_{24}P_4Ru_2S$: C, 37.9; H, 2.45; N, 10.2). Positive-ion FAB mass spectrum: Calc. *m/z* for $C_{52}H_{40}N_{12}F_{18}P_3Ru_2S^+$ ($[(bpy)_2Ru(\mu\text{-dpt})Ru(bpy)_2](PF_6)_3^+$) 1503.0272; found 1503.0253.

The separation and purification of the diastereoisomeric forms were achieved as described previously, however 0.20 mol dm^{-3} sodium benzoate solution was used as the eluent instead of sodium toluene-4-sulfonate solution. Bands 1 (purple) and 2 (brown) were identified as the *rac* and *meso* diastereoisomers,

respectively, as established by ^{1}H NMR and COSY experiments. The ^{1}H NMR spectrum of $[(bpy)_2Ru(\mu\text{-dpt})Ru(bpy)_2](PF_6)_4$ showed the presence of two diastereoisomers, *meso* : *rac* in a ratio of 3 : 1. **Band 1**; *rac* Visible spectrum: λ_{max} (CH_3CN) 530 nm, ε 16 400 M^{-1} cm^{-1}; 421 nm, ε 17 750 M^{-1} cm^{-1}. Electrochemistry (CH_3CN): $E_{1/2}$ = 1421, 1679 mV; for reduction, $E_{1/2}$ = −658 mV (1e), $E_{p,c}$ = −1130 (1e$^-$; irreversible), $E_{1/2}$ = −1333 (1e$^-$), −1386 (1e$^-$), −1621 mV (1e$^-$). ^{1}H NMR (CD_3CN) δ: 7.19, H5b; 7.27, H5d; 7.27, H6b; 7.30, H5c; 7.45, H6d; 7.49, H5-dpt; 7.58, H5a; 7.63, H6c; 7.87, H6-dpt; 7.97, H6a; 8.00, H4d; 8.08, H4c; 8.14, H4b; 8.21, H4-dpt; 8.26, H4a; 8.44, H3d; 8.52, H3b; 8.55, H3c/H3a; 8.92, H3-dpt. **Band 2**; *meso* Visible spectrum: λ_{max} (CH_3CN) 532 nm, ε 16 270 M^{-1} cm^{-1}; 421 nm, ε 17 800 M^{-1} cm^{-1}. Electrochemistry (CH_3CN): $E_{1/2}$ = 1438, 1702 mV; for reduction, $E_{1/2}$ = −722 mV (1e), $E_{p,c}$ = −1194 (1e$^-$; irreversible), $E_{1/2}$ = −1410 (2e$^-$), −1698 mV (1e$^-$). ^{1}H NMR (CD_3CN) δ: 7.32, H5d; 7.36, H5b; 7.45, H5c; 7.49, H6b; 7.55, H6c; 7.61, H5a/H5-dpt; 7.65, H6d; 7.90, H6-dpt; 8.01, H4d; 8.02, H6a; 8.06, H4b; 8.14, H4c; 8.19, H4a; 8.24, H4c-dpt; 8.37, H3b/H3d; 8.57, H3c/H3a; 8.94, H3-dpt {refer to Fig. 9 for numbering system}.

Dichloropalladium(II)-μ-[3,4-di(2-pyridyl)-1,2,5-thiadiazolyl]-bis(2,2′-bipyridine)ruthenium(II) chloride, $[(bpy)_2Ru(\mu\text{-dpt})PdCl_2]Cl_2$. A methanolic solution of 0.1140M $Li_2[PdCl_4]$ (0.45 ml, 0.051 mmol) was added to $[Ru(bpy)_2(dpt)](PF_6)_2$ (44.0 mg, 0.047 mmol) dissolved in refluxing 3 : 1 ethanol–acetone (8 ml). A precipitate formed immediately. Refluxing was continued for 5 min and then the reaction mixture allowed to cool to room temperature and the dark red precipitate collected by filtration and washed with ethanol. Yield 44.7 mg (100%). λ_{max} (CH_3CN) 456 nm, ε 12 000 M^{-1} cm^{-1}. ^{1}H NMR (CD_3CN) δ: 7.51, H5-dpt/4 × H5; 7.68, H3-dpt; 7.86, H4-dpt/H6-dpt/H3′-dpt/H5′-dpt/3 × H6; 8.17, H4′-dpt/4 × H4; 8.38, H6; 8.60, 4 × H3; 9.35, H6′-dpt.

Dichloropalladium(II)-μ-[3,4-di(2-pyridyl)-1,2,5-oxadiazolyl]-bis(4,4′-dimethyl-2,2′-bipyridine)ruthenium(II) chloride, $[(Me_2bpy)_2Ru(\mu\text{-dpo})PdCl_2]Cl_2$. A methanolic solution of 0.0904M $Li_2[PdCl_4]$ solution (0.5 ml, 0.057 mmol) was added to $[Ru(Me_2bpy)_2(dpo)](PF_6)_2$ (22.3 mg, 0.024 mmol) dissolved in refluxing 3 : 1 ethanol–acetone (8 ml). A precipitate formed immediately. Refluxing was continued for 5 min and then the reaction mixture allowed to cool to room temperature and the orange precipitate collected by filtration and washed with ethanol. Yield 22.8 mg (100%). ^{1}H NMR (CD_3CN) δ: 2.56, CH_3; 2.60, CH_3; 2.61, CH_3; 2.63, CH_3; 7.38, 4 × H5; 7.52, H5-dpo; 7.56, H6; 7.61, H6; 7.69, H6; 7.71, H6; 7.85, H3-dpo/H5′-dpo/H6-dpo; 7.93, H4-dpo; 8.06, H3′-dpo; 8.26, H4′-dpo; 8.40, H3; 8.45, 3xH3; 9.33, H6′-dpo.

Dichloro(benzonitrile)palladium(II)-μ-[3,4-di(2-pyridyl)-1,2,5-thiadiazolyl]-bis(2,2′-bipyridine)ruthenium(II) hexafluorophosphate, $[(bpy)_2Ru(\mu\text{-dpt})Pd(PhCN)Cl_2](PF_6)_2$. $[(PhCN)_2PdCl_2]$ (12.7 mg, 0.034 mmol) dissolved in $CHCl_3$ (0.5 ml) was added to $[Ru(bpy)_2(dpt)](PF_6)_2$ (32.2 mg, 0.034 mmol) dissolved in CH_2Cl_2 (1 ml). A precipitate formed immediately and was collected by filtration and washed with $CHCl_3$. Yield 37.8 mg (91%). Positive-ion FAB-MS: Calc. *m*/*z* for $C_{39}H_{30}N_9ClF_6PPdRuS^+$ $\{[(bpy)_2Ru(\mu\text{-dpt})PdCl(NCPh)](PF_6)^+\}$ 1045.9730; found 1045.9758. Visible spectrum: λ_{max} (CH_3CN) 455 nm, ε 13 700 M^{-1} cm^{-1}.

Dichloropalladium(II)-μ-[3,4-di(2-pyridyl)-1,2,5-thiadiazolyl]-bis(2,2′-bipyridine)ruthenium(II) hexafluorophosphate, $[(bpy)_2Ru(\mu\text{-dpt})PdCl_2](PF_6)_2$. Complex $[(bpy)_2Ru(\mu\text{-dpt})PdCl_2](PF_6)_2$ was synthesised by either heating at reflux complex $[(bpy)_2Ru(\mu\text{-dpt})Pd(PhCN)Cl_2](PF_6)_2$ in 3 : 1 ethanol–acetone for 30 min or by combining $[(PhCN)_2PdCl_2]$ (10.1 mg, 0.031 mmol) and complex $[Ru(bpy)_2(dpt)](PF_6)_2$ (30.1 mg, 0.030 mmol) in 3 : 1 ethanol–acetone (4 ml) and heating at reflux for 30 min. After cooling, the solution was taken to dryness *in vacuo*. The solid was re-dissolved in acetone, and diethyl ether was diffused into the solution precipitating a dark red powder (35mg; 90%). The yields were approximately the same for each method. (Found: C, 34.2; H, 1.97; N, 9.7. Calc. for $C_{32}H_{24}N_8Cl_2F_{12}P_2PdRuS$: C, 34.3; H, 2.16; N, 10.0).

(Dimethyl sulfoxide)dichloroplatinum(II)-μ-[3,4-di(2-pyridyl)-1,2,5-thiadiazolyl]-bis(2,2′-bipyridine)ruthenium(II) hexafluorophosphate, $[(bpy)_2Ru(\mu\text{-dpt})Pt(DMSO)Cl_2](PF_6)_2$. The complex $[Ru(bpy)_2(dpt)](PF_6)_2$ (42.3 mg, 0.045 mmol) dissolved in 1 : 1 acetone–ethanol (2 ml) was added to $[(DMSO)_2PtCl_2]$ (19.5 mg, 0.046 mmol) dissolved in nitromethane (0.5 ml), and the resultant solution left overnight. The reaction mixture was then concentrated to dryness *in vacuo*. The residue was re-dissolved in acetone (*ca.* 1 ml) and was filtered through a small plug of celite into a small vial. Vapour diffusion of diethyl ether into this solution precipitated a red powder (53 mg). A sample was examined by positive-ion FAB-MS: Calc. *m*/*z* for $C_{39}H_{30}N_9ClF_6PPdRuS^+$ $([(bpy)_2Ru(\mu\text{-dpt})PtCl_2(DMSO)](PF_6)^+)$ 1142.9693; found 1142.9696. All the remaining material was re-dissolved in 1 : 1 ethanol–nitromethane (4 ml) and refluxed for 8 h. After cooling the same workup procedure was followed. Yield 51 mg (88%). (Found: C, 31.8; H, 2.24; N, 8.9. Calc. for $C_{52}H_{40}N_{12}F_{24}P_4Ru_2S_2$: C, 31.7; H, 2.35; N, 8.7). Visible spectrum: λ_{max} (CH_3CN) 514 nm (ε 7 000 M^{-1} cm^{-1}), 458 nm (ε 11 300 M^{-1} cm^{-1}), 423 nm (ε 11 500 M^{-1} cm^{-1}). Electrochemistry (cyclic voltammetry; CH_3CN): $E_{1/2}$ (Pt^{2+}/Pt^{4+}) = 1410 mV and (Ru^{2+}/Ru^{3+}) = 1670 mV; $E_{1/2}$ for reduction, $E_{p,c}$ = −600 mV (irreversible). ^{1}H NMR (CD_3CN) δ: 2.61, 2 × CH_3; 7.50, 4 × H5; 7.62, H5-dpt; 7.71, H6; 7.74, H6; 7.86, m, H5′-dpt/2 × H6; 7.95, H6-dpt; 8.19, 4 × H4/H4-dpt; 8.50, H4′-dpt; 8.60, 4 × H6; 8.76, H3′-dpt; 8.86, H3-dpt; 9.07, H6′-dpt.

X-Ray crystallography

Crystals of $[Cu(dpt)(NO_3)_2]$ were obtained directly from the reaction mixture, while crystals of $[Ag(dpt)(NO_3)]_n$ were obtained by recrystallisation from acetonitrile. Single crystals of *meso*-$[\{Ru(bpy)_2\}_2(\mu\text{-dpo})][ZnCl_4]_2\cdot 6H_2O$ and *rac*-$[\{Ru(bpy)_2\}_2(\mu\text{-dpo})][ZnCl_4]_2\cdot[ZnCl_2(H_2O)_2]$ were obtained by stirring a suspension of *ca.* 10 mg of the hexafluorophosphate salt in 1 cm^3 distilled water with DOWEX 1 × 8 Cl^- anion exchange resin, to afford the corresponding chloride salt. Following the addition of two molar equivalents of $ZnCl_2$ and aqueous HCl (3 drops, 2 mol dm^{-3}), the solution was allowed to evaporate slowly at room temperature to yield deep red rod-shaped crystals suitable for X-ray determination.

Collection of X-ray diffraction data, solution and refinement of the structures. For all compounds data were collected using a Bruker SMART CCD diffractometer, with total reflections and unique data listed below. Data sets were corrected for absorption using the program SADABS.[52] The structures were solved using direct methods and refined on F^2 using SHELXL97[53] using X-SEED[54] as an interface. All non-hydrogen atoms were located and were refined with anisotropic thermal parameters. Hydrogen atoms were placed in calculated positions (riding model) and were not refined. For the racemic isomer of the binuclear ruthenium complex, the $[ZnCl_2(H_2O)_2]$ molecule was disordered over two sites, but this was successfully refined. Crystal data and a summary of data collection and refinement appear below.

Crystal data for [Cu(dpt)(NO$_3$)$_2$]. $C_{12}H_{58}CuN_6O_6S$, M = 427.84, triclinic, space group $P\bar{1}$ (#2), a = 7.737(2), b = 8.108(2), c = 12.933(3) Å, α = 96.838(3), β = 100.565(3), γ = 102.623(3)°, U = 767.5(3) Å^3, T = 168 K, D_c = 1.851 g cm^{-3} (Z = 2), F(000) = 430, μ(Mo-Kα) = 1.607 mm^{-1}, number of reflections collected =

9879, number of unique reflections = 3113 (R_{int} = 0.0202), $R1$ [$I > 2\sigma(I)$] = 0.0247, $wR2$ (all data) = 0.0654.

Crystal data for [Ag(dpt)(NO$_3$)]$_n$. $C_{12}H_8AgN_5O_3S$, M = 410.16, monoclinic, space group $P2_1/n$ (#14), a = 7.054(2), b = 14,793(4), c = 13.249(4) Å, β = 101.286(3)°, U = 1355.7(7) Å^3, T = 168 K, D_c = 2.010 g cm^{-3} (Z = 4), F(000) = 808, μ(Mo-Kα) = 1.661 mm^{-1}, number of reflections collected = 17123, number of unique reflections = 2584 (R_{int} = 0.0374), $R1$ [$I > 2\sigma(I)$] = 0.0318, $wR2$ (all data) = 0.0778.

Crystal data for meso-[(bpy)$_2$Ru(μ-dpo)Ru(bpy)$_2$][ZnCl$_4$]$_2$·6H$_2$O. $C_{52}H_{52}Cl_8N_{12}O_7Ru_2Zn_2$, M = 1573.54, monoclinic, space group $P2_1/n$ (#14), a = 13.743(3), b = 21.685(4), c = 21.332(4) Å, β = 92.55(3)°, U = 6531(2) Å^3, T = 195 K, D_c = 1.6469 g cm^{-3} (Z = 4), F(000) = 3152, μ(Mo-Kα) = 1.607 mm^{-1}, number of reflections collected = 40153, number of unique reflections = 14867 (R_{int} = 0.0053), $R1$ [$I > 2\sigma(I)$] = 0.0566, $wR2$ (all data) = 0.1815.

Crystal data for rac-[(bpy)$_2$Ru(μ-dpo)Ru(bpy)$_2$][ZnCl$_4$]$_2$·[ZnCl$_2$(H$_2$O)$_2$]. $C_{52}H_{44}Cl_{10}N_{12}O_3Ru_2Zn_3$, M = 1637.74, triclinic, space group, $P\bar{1}$ (#2), a = 14.855(2), b = 16.198(2), c = 17.717(3) Å, α = 75.475(3), β = 66.629(3), γ = 70.992(3)°, U = 3663.4(9) Å^3, T = 195 K, D_c = 1.485 g cm^{-3} (Z = 2), F(000) = 1624, μ(Mo-Kα) = 1.78 mm^{-1}, number of reflections collected = 24743, number of unique reflections = 16968 (R_{int} = 0.069), $R1$ [$I > 2\sigma(I)$] = 0.0805, $wR2$ (all data) = 0.2822.

CCDC reference numbers 182547–182550.

See http://www.rsc.org/suppdata/dt/b2/b202954e/ for crystallographic data in CIF or other electronic format.

Acknowledgements

We thank the Australian Research Council and the Royal Society of New Zealand Marsden Fund for financial support of this work.

References

1 V. Balzani and F. Scandola, *Supramolecular Photochemistry*, Ellis Horwood, Chichester, UK, 1991.
2 J. P. Sauvage, *Acc. Chem. Res.*, 1998, **31**, 611–619.
3 V. Balzani, A. Juris, M. Venturi, S. Campagna and S. Serroni, *Chem. Rev.*, 1996, **96**, 759–833.
4 X. Hua and A. von Zelewsky, *Inorg. Chem.*, 1995, **34**, 5791–5797.
5 I. G. Phillips and P. J. Steel, *Aust. J. Chem.*, 1998, **51**, 371–382.
6 G. Denti, S. Campagna, L. Sabatino, S. Serroni, M. Ciano and V. Balzani, *Inorg. Chem.*, 1990, **29**, 4750–4758.
7 V. K. Bel'skii, O. G. Ellert, Z. M. Seifulina, V. M. Novotortsev, V. S. Tseveniashvili and A. D. Garnovskii, *Izv. Akad. Nauk SSSR, Ser. Khim.*, 1984, 1914–1915.
8 M. Munakata, T. Kuroda-Sowa, M. Maekawa, N. Nakamura, S. Akiyama and S. Kitagawa, *Inorg. Chem.*, 1994, **33**, 1284–1291.
9 A. F. Hill, A. J. P. White, D. J. Williams and J. D. E. T. Wilton-Ely, *Organometallics*, 1998, **17**, 4249–4258.
10 L. G. Kuz'mina, L. P. Grigor'eva, Y. T. Struchkov, Z. I. Ezhkova, B. E. Zaitsev, V. V. Davidov and A. K. Molodkin, *Zh. Neorg. Khim.*, 1980, **25**, 2931–2938.
11 C. R. Stoner, A. L. Rheingold and T. B. T. B. Brill, *Inorg. Chem.*, 1991, **30**, 360–364.
12 K. Skorda, G. S. Papaefstathiou, A. Vafiadis, A. Lithoxoidou, C. P. Raptopoulou, A. Terzis, V. Psycharis, E. Bakalbassis, V. Tangoulis and S. P. Perlepes, *Inorg. Chim. Acta*, 2001, **326**, 53–64.
13 W. Kaim, S. Kohlmann, A. J. Lees and M. Zulu, *Z. Anorg. Allg. Chem.*, 1989, **575**, 97–114.
14 M. Munakata, H. He, T. Kuroda-Sowa, M. Maekawa and Y. Suenaga, *J. Chem. Soc., Dalton Trans.*, 1998, 1499–1502.
15 R. M. Paton, in *Comprehensive Heterocyclic Chemistry*, eds. A. R. Katritzky, C. W. Rees and E. F. V. Scriven, Pergamon, Oxford, 1996, p. 220; and references therein.
16 I. Shinkai and P. J. Reider, in *Comprehensive Heterocyclic Chemistry*, eds. A. R. Katritzky, C. W. Rees and E. F. V. Scriven, Oxford, 1996, p. 335.
17 L. M. Weinstock, P. Davis, B. Handlsman and R. Tull, *J. Org. Chem.*, 1967, **32**, 2823–2829.
18 X.-G. Duan, X.-L. Duan, C. W. Rees and T.-Y. Yue, *J. Heterocycl. Chem.*, 1996, **33**, 1419–1427.
19 X.-G. Duan, X.-L. Duan, C. W. Rees and T.-Y. Yue, *J. Chem. Soc., Perkin Trans. 1*, 1997, 2597–2602.
20 X.-G. Duan and C. W. Rees, *J. Chem. Soc., Perkin Trans. 1*, 1997, 3189–3196.
21 C. W. Rees and T.-Y. Yue, *Chem. Commun.*, 1998, 1207–1208.
22 C. W. Rees and T.-Y. Yue, *J. Chem. Soc., Perkin Trans. 1*, 2001, 662–667.
23 C. W. Rees and T.-Y. Yue, *J. Chem. Soc., Perkin Trans. 1*, 2001, 2538–2542.
24 C. Richardson and P. J. Steel, *Acta Crystallogr., Sect. C*, 2001, **57**, 197–198.
25 G. R. Newkome and D. L. Koppersmith, *J. Org. Chem.*, 1973, **38**, 4461–4463.
26 A. Juris, S. Barigelletti, S. Campagna, V. Balzani, P. Belser and A. von Zelewsky, *Coord. Chem. Rev.*, 1988, **84**, 85–277.
27 G. P. Bean, *J. Org. Chem.*, 1998, **63**, 2497–2506.
28 F. R. Keene, *Coord. Chem. Rev.*, 1997, **166**, 122–159.
29 C. Richardson and P. J. Steel, *Aust. J. Chem.*, 2000, **53**, 93–97.
30 M. Munakata, L. P. Wu and T. Kuroda-Sowa, *Adv. Inorg. Chem.*, 1999, **46**, 173–303.
31 C. M. Hartshorn and P. J. Steel, *J. Chem. Soc., Dalton Trans.*, 1998, 3935–3940.
32 F. R. Keene, *Chem. Soc. Rev.*, 1998, **27**, 185–193.
33 M.-A. Haga, M. M. Ali, S. Koseki, A. Yoshimura, K. Nozaki and T. Ohno, *Inorg. Chim. Acta*, 1994, **226**, 17–24.
34 L. S. Kelso, D. A. Reitsma and F. R. Keene, *Inorg. Chem.*, 1996, **35**, 5144–5153.
35 D. M. D'Alessandro, L. S. Kelso and F. R. Keene, *Inorg. Chem.*, 2001, **40**, 6841–6844.
36 C. Creutz, *Prog. Inorg. Chem.*, 1983, **30**, 1–73.
37 F. Dejehet, R. Debuyst and J. P. Declercq, *J. Chim. Phys., Phys-Chim. Biol.*, 1986, **83**, 85–90.
38 S. Ernst, V. Kasack and W. Kaim, *Inorg. Chem.*, 1988, **27**, 1146–1148.
39 S. D. Ernst and W. Kaim, *Inorg. Chem.*, 1989, **28**, 1520–1528.
40 K. Kalyanasundaram and M. K. Nazeeruddin, *Inorg. Chem.*, 1990, **29**, 1888–1897.
41 D. P. Rillema, R. Sahai, P. Matthews, A. K. Edwards, R. J. Shaver and L. Morgan, *Inorg. Chem.*, 1990, **29**, 167–175.
42 V. W.-W. Yam, V. W.-M. Lee and K.-K. Cheung, *J. Chem. Soc., Chem. Commun.*, 1994, 2075–2076.
43 W. L. Jolly and K. D. Maguire, *Inorg. Synth.*, 1967, **9**, 102–111.
44 G. G. Alange, A. J. Banister and B. Bell, *J. Chem. Soc., Dalton Trans.*, 1972, 2399–2400.
45 T. Togano, N. Nagao, M. Tsuchida, H. Kumakura, K. Hisamatsu, F. S. Howell and M. Mukaida, *Inorg. Chim. Acta*, 1992, **195**, 221–225.
46 P. A. Mabrouk and M. S. Wrighton, *Inorg. Chem.*, 1986, **25**, 526–531.
47 I. P. Evans, A. Spencer and G. Wilkinson, *J. Chem. Soc., Dalton Trans.*, 1973, 204–209.
48 R. F. Heck, *Palladium Reagents in Organic Synthesis*, Academic Press, London, 1985.
49 J. H. Price, A. N. Williamson, R. F. Schramm and B. B. Wayland, *Inorg. Chem.*, 1972, **11**, 1280–1284.
50 N. C. Fletcher, P. C. Junk, D. A. Reitsma and F. R. Keene, *J. Chem. Soc., Dalton Trans.*, 1998, 133–138.
51 N. C. Fletcher and F. R. Keene, *J. Chem. Soc., Dalton Trans.*, 1999, 683–689.
52 R. H. Blessing, *Acta. Crystallogr., Sect. A*, 1995, **51**, 33–38.
53 G. M. Sheldrick, in SHELXL-97, University of Göttingen, Göttingen, Germany, 1997.
54 L. J. Barbour, in X-SEED Crystallographic Interface, University of Missouri, Columbia, MO, USA, 1999.